Accepted Manuscript

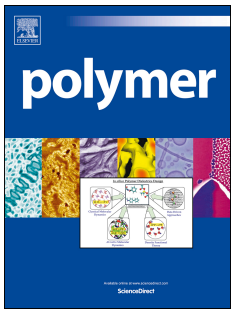

UV-converting blue-emitting polyfluorene-based organic-inorganic hybrids for solid state lighting

Thays C.F. Santos, Rebeca R. Rodrigues, Sandra F.H. Correia, Luís D. Carlos, Rute A.S. Ferreira, Celso Molina, Laura O. Péres

PII: S0032-3861(19)30363-5

DOI: https://doi.org/10.1016/j.polymer.2019.04.042

Reference: JPOL 21425

To appear in: *Polymer*

Received Date: 20 February 2019

Revised Date: 16 April 2019

Accepted Date: 18 April 2019

Please cite this article as: Santos TCF, Rodrigues RR, Correia SFH, Carlos LuíD, Ferreira RAS, Molina C, Péres LO, UV-converting blue-emitting polyfluorene-based organic-inorganic hybrids for solid state lighting, *Polymer* (2019), doi: https://doi.org/10.1016/j.polymer.2019.04.042.

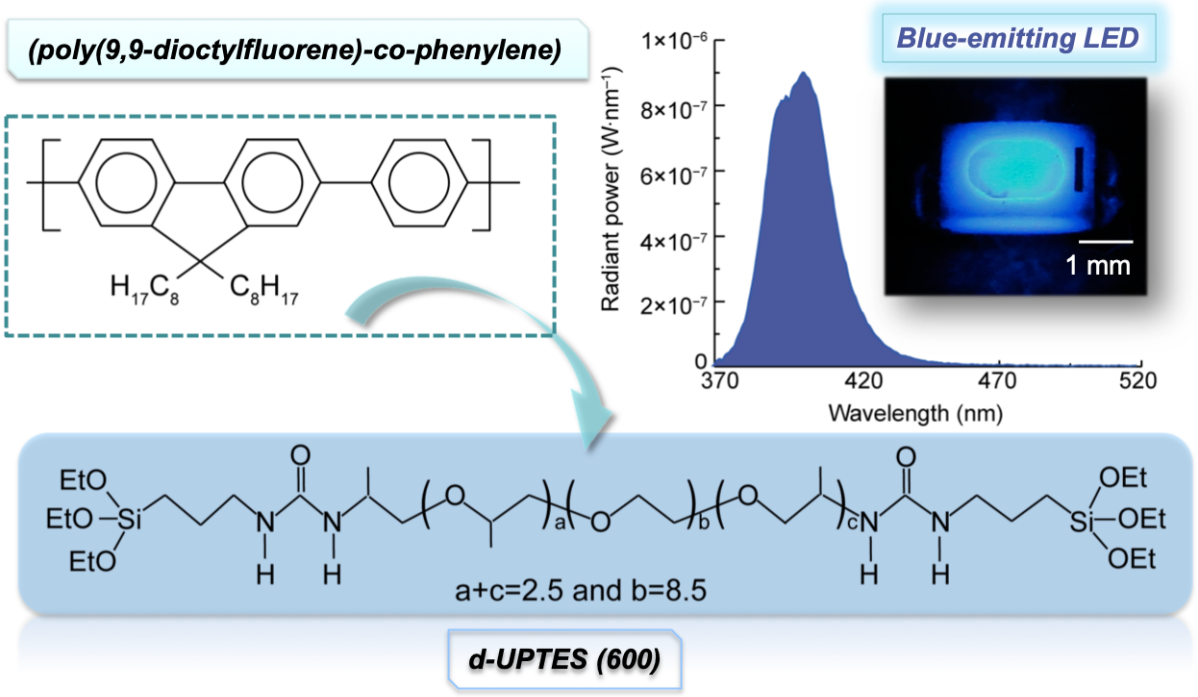

UV-converting blue-emitting polyfluorene-based organic–inorganic hybrids for solid state lighting

Thays C. F. Santos[1], Rebeca R. Rodrigues[1], Sandra F. H. Correia[2], Luís D. Carlos[2], Rute A. S. Ferreira[2*], Celso Molina[1*], Laura O. Péres[1]

[1]Department of Chemistry, Federal University of São Paulo (UNIFESP), Diadema-SP, Brazil

[2]Departamento de Física and CICECO – Aveiro Institute of Materials, Universidade de Aveiro, 3810-193 Aveiro, Portugal

Abstract

Solid state lighting (SSL) revolutionized the light sources and displays market. Challenges include the seek for low cost and efficient materials able to emit pure colours (red, green and blue). Herein, we report amine-functionalized organic/inorganic di-ureasil hybrids consisting of a siliceous skeleton and oligopolyether chains, d-U(600), modified by distinct concentration values of a blue emitting uncharged polyfluorene (poly(9,9-dioctylfluorene)-co-phenylene) (PF). Structural and thermal studies reveal that the interaction between the PF and the d-U(600) yield to an enhancement of the PF thermal stability. The optical characterization shows that the emission is strongly dependent on the excitation energy presenting a red-shift as the excitation wavelength increases, enabling a fine tuning of the emission color coordinates. Under UV excitation, a maximum emission quantum yield value 0.44±0.04 was attained, which is remarkably higher when compared to the value found for the undoped d-U(600), 0.13±0.01, an analogous to the value found for the isolated PF, pointing out that the incorporation into the hybrid host did not yield to an emission efficiency quenching. A commercial LED chip emitting at 365 nm was coated by the PF-doped d-U(600) showing a wall-plug efficiency of 0.04% and a luminous efficacy of 0.003 $lm \cdot W^{-1}$, demonstrating the applicability of these materials as blue-emitting phosphors to be applied in SSL.

Keywords: di-ureasil; light-emitting diode; conjugated polymer

*Corresponding authors: cmolina@unifesp.br; Tel. +55 (11) 40440500, R: 3568

rferreira@ua.pt; Tel. +351 234 378 103

1. Introduction

Polyfluorenes (PFs) with di-substitution at 9-position were the first conjugated polymers (CP) displaying simultaneously good solubility and efficient emission in the blue spectral region [1,2]. This emission can be modulated inserted some chromophore, like phenylene, pyridine, anthracene and thiophene, in the fluorene group or by producing copolymers in the backbone of the main chain [3-9]. This class of materials has been widely used in the development of electroluminescent devices due to its interesting properties, such as chemical, thermal and oxidative stability [10-13].

However, the potential degradation of the material, such as, for instance, induced by the oxidation of the conjugated chain, affects the applicability and devices' performance. For PFs, this effect is known as "keto defect", producing the 9-fluorenone, and can be identified by an emission at 2.2 eV and a vibrational band at 1721 cm^{-1} [14,15]. The formation of the "keto defect" is the result of oxidation processes. Chakraborty *et al.* produced a hybrid material using a cationic PF intercalated in kaolinite clay. Their results shows that the "keto defect" sites of PFs are significantly reduced, suggesting that the intercalation is a good way to protect the polymer [16]. In fact, the insertion of the polymer in a matrix, like a non-conjugated polymer or an inorganic compound, can improve and protect the material, which enables better arrangement of his chain and consequently, enhanced emission properties [4,11,17,18]. However, the use of only inorganic components promotes aggregates and phase separation affecting the structure and the optical properties of the final material, limiting, therefore, practical applications. In order to overcome this

drawback, organic-inorganic hybrid matrices appear as an alternative approach. The advantage of organic-inorganic hybrids lies on the fact that they are easily processed at room temperature with the desired shape and thickness, combining the flexibility of the organic counterpart with the mechanical stability of the inorganic one [19-21].

The intercalation of conjugated polymers in organic-inorganic hybrid hosts can be obtained by the insertion of the polymer after the synthesis of the inorganic component. However, this process may require high pressure or temperature which can promote oxidation of the CP [22]. An alternative approach is to insert *in-situ* the conjugated material during the preparation of the hybrid itself.

Among the different organic-inorganic hybrids materials, di-ureasils appear as good choice, accordingly to recent reports. For instance, Evans *et al.* [23,24] reported a photoluminescent material based on a di-ureasil, the d-U(600), containing a PF, poly(*p*-phenylene vinylene), and polythiophene. In these studies, even using very long synthetic routes, the authors used charged polymers to improve solubility and, consequently, the interaction between the CP and the inorganic material. Moreover, this d-U(600) host material has been investigated for several applications, such as luminescent solar concentrators [25-28], QR codes [29] and optoelectronic devices [30].

Solid-state lighting (SSL) is based on white light-emitting diodes (WLEDs) based on UV/vis-downshifting materials [31-33]. The most efficient WLED is a combination of a blue LED chip and YAG:Ce^{3+} yellow-emitting phosphor which, nevertheless, presented a poor color rendering index (CRI) due to the lack of the red component [34]. One possible approach to improve the CRI is to use red, green, and blue broadband-emitting phosphors with a shorter-wavelength (UV)-emitting LED [32]. Thus, the development of several blue-

emitting phosphors has been reported [32,35-37], showing their applicability to UV-converting WLEDs [31,33,37].

Here, a soluble uncharged PF (poly(9,9-dioctylfluorene)-co-phenylene) was incorporated into d-U(600), and so-called d-U(600)/PF, and its structural and luminescent properties were investigated. Taking advantage of the demonstrated efficient UV downshifting conversion ability of the d-U(600)/PF films, an UV-emitting LED coated with the hybrid material, presenting a maximum wall-plug efficiency and luminous efficacy of 0.04% and 0.003 $lm \cdot W^{-1}$, respectively. These results are a proof of concept for the applicability of PF-doped organic-inorganic hybrids for the fabrication of UV-pumped WLEDs based on the superposition of red, green and blue-emitting phosphors.

2. Experimental Section

Materials. Potassium carbonate (CAAL, 99%), 1,4-phenylene bisboronic (Aldrich, 96%), 9,9'-dioctyl-2,7-dibromofluorene (Aldrich, 96%), phenylboronic acid (Aldrich, 99%), xylene (Synth 98.5%), tetrakis(triphenylphosphine) palladium (Aldrich, 99%), chloroform (CAAL, 99%), methanol (Synth 99.8%), hydrogen peroxide (CAAL, 35%), Jeffamine® ED-600 (Aldrich, 97%), isocyanatepropyltriethoxysilane (ICPTES, Fluka, 95%) and tetrahydrofuran (THF) (Synth, 99%), (n-butanol anhydrous, Sigma-Aldrich, 99.8%) were used without purification.

Syntheses of polyfluorene (PF). The poly(9,9-dioctylfluorene)-co-phenylene was synthesized by Suzuki reaction, as described in the literature [5,38], using 9,9-dioctylfluorene-2,7-dibromofluorene, 1,4-phenylenebisboronic acid and tetrakis-(triphenylphosphine) palladium, $P(Ph_3)_4Pd$, as a catalyst. The material obtained was

washed with water and hydrogen peroxide, and then recrystallized in methanol, when a yellow viscous material was obtained with yield of 87%. Mn=4.19×10^3 g·mol^{-1}, Mw=4.76×10^3g·mol^{-1}, Mw/Mn=1.14. The material was prepared in a one-way step, with high yield, forming a polymer very soluble in common organic solvents. The structure was confirmed by ^{1}H NMR spectrum (support information).

di-ureapropyltriethoxysilane (d-UPTES). The synthesis of the non-hydrolyzed organic-inorganic hybrid precursor, d-UPTES, has been described in detail elsewhere [39,40]. All the chemicals used in the synthesis were purchased from Fluka and Aldrich and used as received. Typically, the commercially named Jeffamine® ED-600 polyetheramine containing NH_2 groups reacts with ICPTES in a molar ratio ICPTES:Jeffamine 2:1 in THF under reflux and stirring at 80 °C for 24 hours. The precursor was obtained after evaporating the solvent in a rotary bench evaporator.

Synthesis of d-U(600) and PF-doped hybrids. The d-UPTES precursor was diluted in n-butanol and then HCl 0.01 mol·L^{-1} was added in a ratio UPTES:butanol:HCl=1:10:0.1 (w:v:v) to promote hydrolysis reactions. The *sol* was kept under magnetic stirring for 24 h to obtain a rubbery d-U(600) pristine gel in a monolith wet form. For the PF-doped d-U(600) hybrids, the same experimental procedure was adopted including different PF content in a ratio d-UPTES:PF of 1:0.01, 1:0.05, 1:0.10 and 1:0.20 (w:w) and labeled as d-U(600) (pristine hybrid) and d-U(600)PF_x to those containing PF (where x=1, 5, 10 and 20, respectively). Monoliths were kept at room temperature for eleven days, being the optimum time period for aging, followed by an heat treatment at 50 °C for 24 h, at 80 °C for 48 h, at 110 °C for 1h and finally at 120 °C for another 1 h in an oven under vacuum conditions. We note that in the d-U(600)PF_x samples, the hybrid matrix promotes a transparent and

flexible material, whereas the presence of PF induced opacity, as a function of the polymer content. However, in all cases, it was possible to obtain a homogenous material, but less flexible as the PF concentration increases. All the optical measurements were performed with samples in solid state in a monolith form.

Fourier-transform infrared (FT-IR). The spectra were acquired at room temperature on a ShimadzuIRPrestige-21 with a spectral resolution of 4 cm^{-1} and 128 scans in the frequency range 4000-500 cm^{-1}. The samples were measured in KBr pellets.

Thermogravimetry. The thermogravimetry (TG) measurements were performed using a DTG-60 Shimadzu equipment. The measures were carried out using approximately 5 mg of material at inert nitrogen atmosphere (200 $mL \cdot min^{-1}$), range of 30 to 800 ^{o}C at 10 $^{o}C \cdot min^{-1}$.

***Gel permeation chromatography*.** The molar mass and the polydispersity were determined by gel permeation chromatography (GPC) using a Waters HPLC system that comprised two columns in series (i.e., a PLgel mixed-B and a PLgel mixed-C) at 35 °C and with THF used as the eluent at a flow rate of 1 $mL \cdot min^{-1}$. GPC measurements were performed using monodisperse polystyrene samples as standards.

Photoluminescence. The emission and excitation spectra were recorded at room temperature with a modular double grating excitation spectrofluorimeter with a TRIAX 320 emission monochromator (Fluorolog-3, Horiba Scientific) coupled to a R928 Hamamatsu photomultiplier, using a front face acquisition mode. The excitation source was a 450 W Xe arc lamp. The emission spectra were corrected for detection and optical spectral response of the spectrofluorimeter and the excitation spectra were corrected for the spectral distribution of the lamp intensity using a photodiode reference detector.

Absolute emission quantum yield (q). The measurements were performed at room temperature using a quantum yield measurement system C9920-02 from Hamamatsu with a 150 W Xenon lamp coupled to a monochromator for wavelength discrimination, an integrating sphere as sample chamber and a multi-channel analyser for signal detection. Three measurements were made for each sample so that the average value is reported. The method is accurate to within 10 %.

LED characterization. The radiant power spectra were recorded using an integrating sphere (ISP 150L, Instrument Systems) connected to a detector (MAS40-121, Instrument Systems), with an integration time of 10 s. The emission colour coordinates were calculated from the emission spectra using the 1931 Commission Internationale de Éclairage (CIE) methodology defined for the 2º standard.

3. Results and Discussion

Structural properties

The electrostatic interaction between the d-U(600) host and PF was studied by FT-IR spectroscopy (Figure 1(a) and Figure S2 and Table S1 in ESI). Emphasis was given to the analysis of the amide I (1700-1600 cm^{-1}) region [39]. The hydrogen bonding in this region arises from interactions between urea groups of different chains of d-U(600) and between bonded urea groups and the PEO chains [39,40]. The amide I region provides information about the degree of hydrogen bonding interactions, mainly associated with $\nu_{C=O}$ (1637 cm^{-1}), Figure 1 and Figure S2 in ESI, which are involved in more ordered hydrogen-bonded urea-urea associations [39,40]. The absence of the peak at 1750 cm^{-1} in the d-U(600)PF_x hybrids indicates there are no free urea groups (not associated to hydrogen

bonds). After the incorporation of PF, two contribution are discerned around 1719 cm^{-1} (1) and 1669 cm^{-1} (2) attributed to disordered hydrogen bonding polyether/urea [39,40]. The position of the energetic peak of amide I remains constant nearly 1637 cm^{-1} (3) indicating that the urea–urea aggregates are unaffected as the polymer concentration increases. The small shifting to higher wavenumber of band (1) reveals interactions between PF and hybrid matrix in the urea/polyether region probably due to weak intermolecular forces such as dipole–induced type once there is no charge on the PF. Although this interaction can be observed, this band remains practically unchanged for the entire range of PF incorporated. The constant contribution of this band as a function of the PF indicates that residual fluorenone species are not present [41]. Figure 1(b) shows the composition dependence of the integrated area of the resolved components for each FT-IR component labelled as (1), (2) and (3) as a function of the % polymer content. For d-U(600)PF_1, the component at 1719 cm^{-1} presents a slight enhancement when compared with that of d-U(600), revealing an increase of this contribution to the poly(oxyethylene)/urea disordered hydrogen bonding. At d-U(600)PF_5, a larger enhancement of the contribution at 1669 cm^{-1} and a decrease of the component at 1637 cm^{-1} are observed. This suggests that PF, in this concentration, is interacting more effectively in the urea/urea hydrogen bonding and can be related to the higher quantum yield obtained and discussed further on. For the highest PF concentration, from 10 to 20%, the bands appear to be unaffected. The low interaction between the CP and the hybrid host in good agreement with previous studies on charged CP inserted into d-U(600) [23,24] and also on uncharged n *p*-terphenyl, *p*-quaterphenyl, and *p*-sexiphenyl [42].

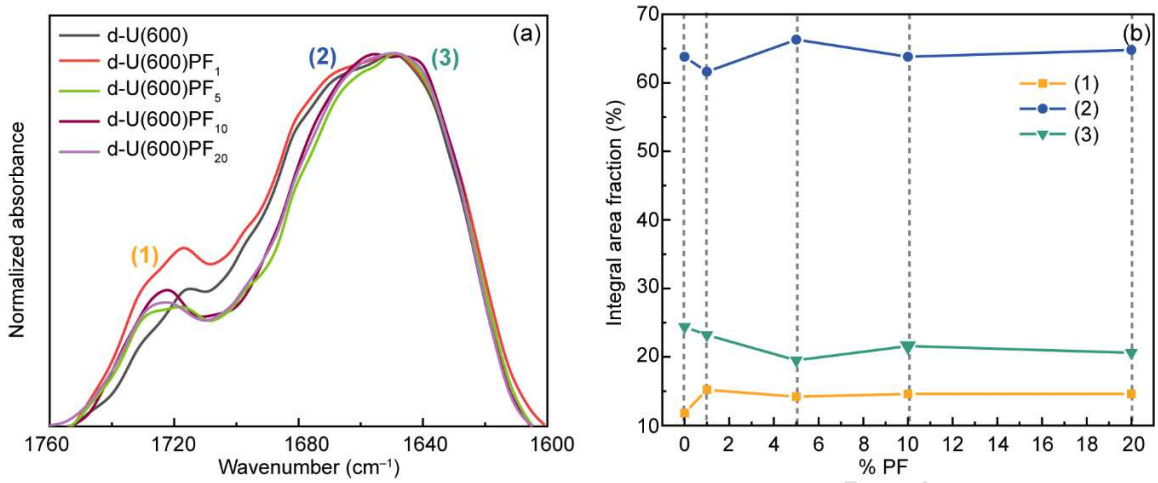

Figure 1. (a) FT-IR spectra of d-U(600) and d-U(600)PF_x (x=1 to 20) in the amide I region and (b) % PF dependence of the integral area fraction (%) of the curve fitting components (1) 1719; (2) 1669 and (3) 1637 cm^{-1}.

A relevant aspect resulting from the PF interaction with the hybrid host is the thermal stability of the d-U(600)-PF_x featuring SSL applications. Figure 2 shows the TGA and DrTGA curves and Table S2 in ESI presents the percentage of mass loss for PF, d-U(600) and d-U(600)PF_x samples. For PF it is possible to observe an event at approximately 80 ^oC due to the elimination of the water/solvents. The TG curves exhibit two major events at 255 ^oC and 355 ^oC attributed, respectively, to the loss of side chains attached to the polymer backbone and to the decomposition of the backbone [41]. The rigid structure of the polymer (with one phenylene and fluorene group) lost basically all its mass until 500 ^oC. When incorporated into the d-U(600), it is possible to observe that the materials lose approximately 80% of their mass up to 800 ^oC. We note that the d-U(600)-based materials reveal an increase of the initial temperature (T_{onset}), comparing with pristine

PF, pointing out that the hybrid host can improve the stability of the conjugated polymer, protecting it against degradation.

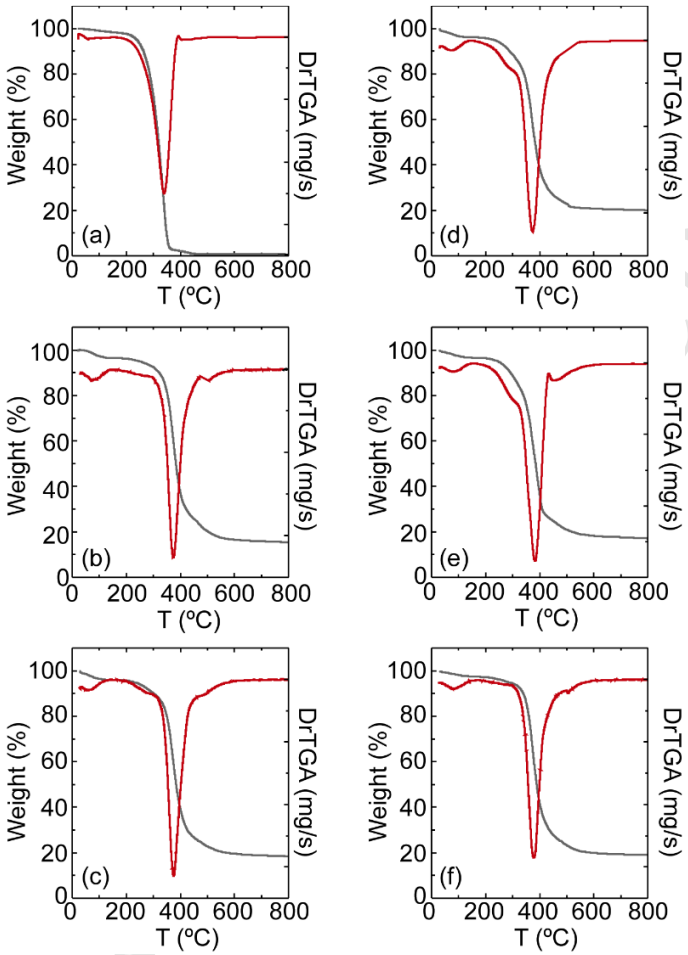

Figure 2. TGA and DrTGA curves of (a) PF, (b) d-U(600)PF_1, (c) d-U(600)PF_5, (d) d-U(600)PF_{10}, (e) d-U(600)PF_{20} and (f) d-U(600).

Optical properties

The emission spectra of d-U(600)PF_x reveal a broad emission in the blue spectral region, Figure 3(a), with two main components in the blue/green spectral regions, independently of the PF concentration and of the excitation wavelength (Figures S3-S6 in ESI). The band results from the synergetic contribution of the d-U(600) intrinsic emission

[22, 41] with that of the isolated PF [18], Figure 3(b). We notice that the emission red shift as the PF amount increases is due to the larger contribution of the polymer emitting states (Figure 3b).

The interaction between the d-U(600) hybrid and the PF is evidenced in the analysis of the excitation spectra monitored at the polymer-related emission (around 450 nm), as function of the PF concentration and of the monitoring wavelength (Figure 3c and Figures S3-S6 in ESI). At lower PF concentrations, d-U(600)PF_1, the spectrum reveals two main components at around 280 nm and 340 nm. These excitation components overlap the excitation spectra of the isolated d-U(600) and PF, disabling a selective analysis of its origin. Nonetheless, the increase of the relative intensity of the low-wavelength component (280 nm) as the PF concentration increases, suggests that this band is mainly originated from the polymer-related excited states, Figures 3(c) and (d). The contribution of the PF excited states at higher polymer concentrations is also evidenced by the red-shift of the higher wavelength one from 340 nm to 365 nm due to the contribution of the low-relative band observed in the excitation of the pure PF.

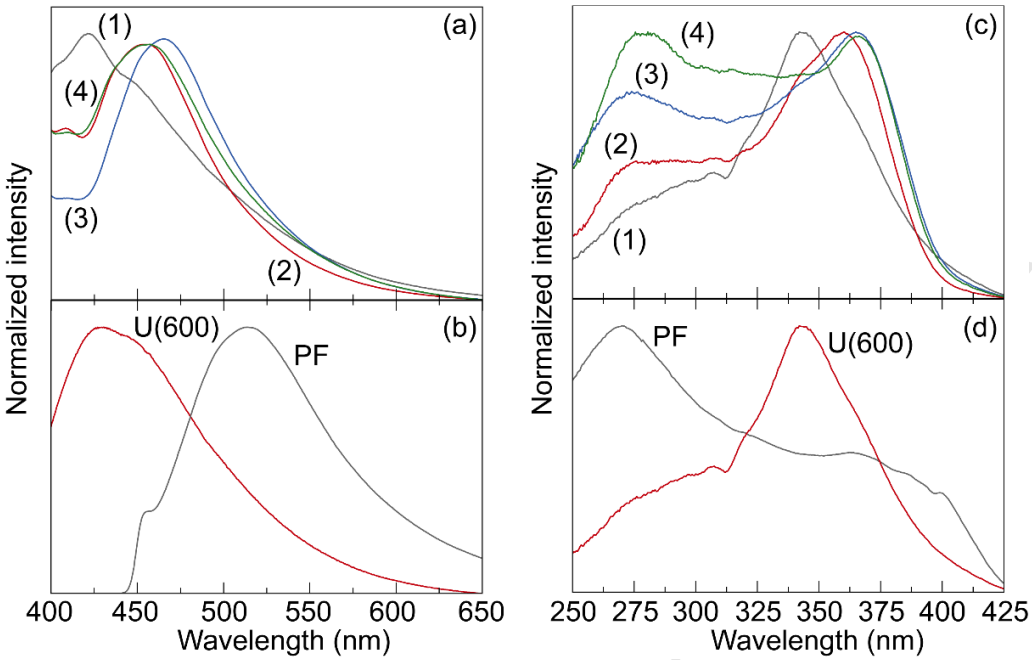

Figure 3. Emission spectra of (a) d-U(600)PF_1 (1), d-U(600)PF_5 (2), d-U(600)PF_{10} (3) and d-U(600)PF_{20} (4) and (b) PF and undoped d-U(600) excited at 365 nm; excitation spectra of the (c) d-U(600)PF_1 (1), d-U(600)PF_5 (2), d-U(600)PF_{10} (3) and d-U(600)PF_{20} (4) and of the (d) PF and undoped d-U(600) monitored at 450 nm.

The absolute emission quantum yield (q) values were measured as a function of the PF concentration and excitation wavelength, namely preferentially excitation into the PF- (280 nm) and d-U(600)- related states (340-365 nm). Table 1 shows the q values for the excitation wavelength that maximises the emission intensity (Figure 3(c)). The d-U(600) sample exhibits a constant (within the experimental error) value of 0.13±0.01, for 340-365 nm excitation (Table S3), in good agreement with previously reported values [43]. A notable increase in the q value is observed for the d-U(600)-PF_x samples, the highest value reaching 0.43±0.04 for d-U(600)PF_5 (analogous to the value recorded for the pure polymer, Table 1 and reference [44]).

Table 1. Absolute emission quantum yield (*q*) values for the fabricated samples. The excitation wavelength is also indicated.

Sample	*q*
PF	0.43±0.04 (365 nm)
d-U(600)	0.13±0.01 (340 nm)
d-U(600)PF$_1$	0.26±0.03 (340 nm)
d-U(600)PF$_5$	0.43±0.04 (365 nm)
d-U(600)PF$_{10}$	0.32±0.03 (365 nm)
d-U(600)PF$_{20}$	0.41±0.04 (365 nm)

One of the main processes affecting the *q* values of conjugated polymers is the quenching of excitons at non-emissive defect sites [45]. By increasing the PF concentration, aggregation may occur, increasing the rate of exciton migration and, thus, leading to a decrease in *q* due to trapping at these sites. However, as the most concentrated sample, d-U(600)PF$_{20}$, presented values similar to those of d-U(600)PF$_5$, PF aggregation if effective might only play some rule in the d-U(600)PF$_{10}$ hybrid.

All the fabricated d-U(600)PF$_x$ samples presented a bluish emission, regardless of the PF concentration, as shown in the Commission International de l'Eclairage (CIE) diagram in Figure 4(a) and of the used excitation wavelength range, Figure 4(b).

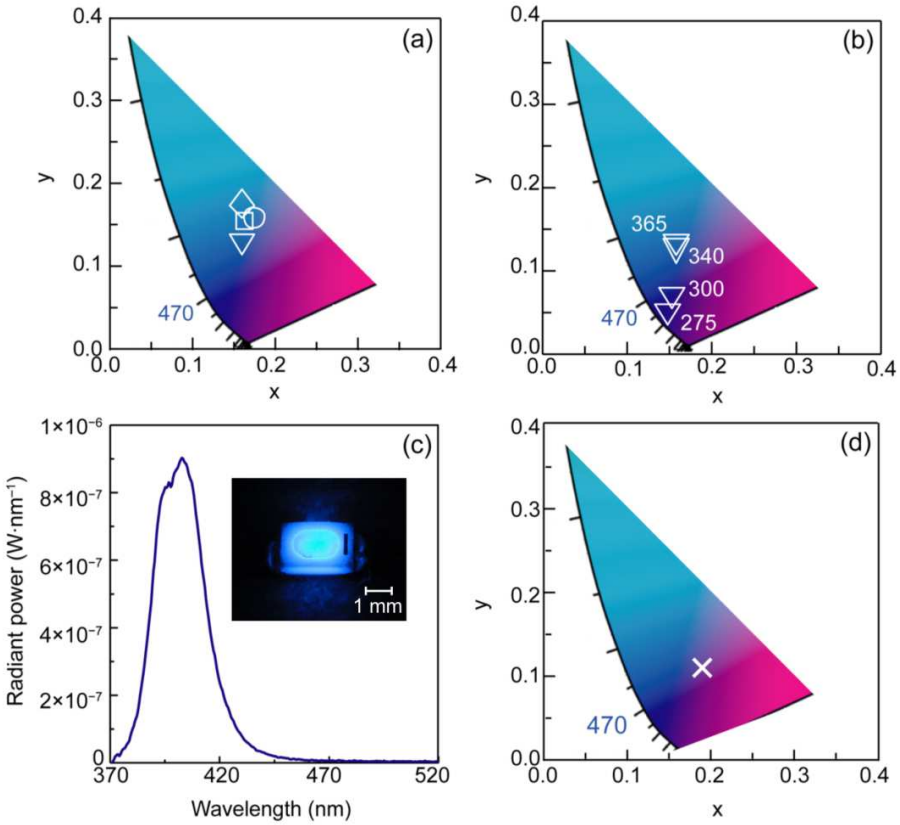

Figure 4. (a) The 1931 Commission International de l' Eclairage (CIE) chromaticity diagram showing the (x,y) emission colour of d-U(600)PF_1(circle), d-U(600)PF_5 (triangle), d-U(600)PF_{10} (diamond) and d-U(600)PF_{20} (square) excited at 365 nm and (b) of d-U(600)PF_5 as function of the excitation wavelength indicated for each data point, in nm; (c) radiant power spectrum of the best performance device; (d) CIE chromaticity diagram showing the (x,y) emission colour of the fabricated LED operating on 3.5 V; 20 mA. The inset shows a photograph of the LED.

Properties of the LED device

Taking advantage of the blue emission with high *q* value, the d-U(600)PF_5 material was used to produce a blue-emitting LED device by coating a commercial UV-emitting chip (365 nm). The radiant power spectrum of the best performance device is presented in

Figure 4(c), revealing a broad band in the blue similar to that measured for the d-U(600)PF_5 (Figure 3). The LED performance was characterized by the estimation of the wall-plug efficiency (ratio between the radiant and the electrical powers) and the luminous efficacy (ratio between the luminous flux and the electrical power) yielding values of 0.04% and 0.003 $lm \cdot W^{-1}$, respectively. Figure 4(d) shows the 1931 CIE chromaticity diagram for the fabricated device, showing an emission in the UV-blue region, in good agreement with the calculated color coordinates for d-U(600)PF_5 presented in Figure 4(b).

4. Conclusions

Novel organic-inorganic hybrid materials based on uncharged polyfluorene and the d-U(600) di-ureasil hybrid, were prepared. Structural results pointed out an effective interaction between the polymer and the hybrid host, leading to enhanced thermal stability and maximum absolute emission quantum yield value of 0.44±0.04, obtained at lower PF doping concentrations (5% w/w). The organic-inorganic hybrid host provided additional advantages, such as preventing aggregation and clustering, which typically yield as non-radiative channels. A UV-downshifting blue-emitting LED device was produced with a wall-plug efficiency and a luminous efficacy of 0.04% and 0.003 $lm \cdot W^{-1}$, respectively, demonstrating that the proposed hybrids can be used as a blue emitting downshifting phosphors for UV-pumped WLEDs.

Acknowledgements

The authors would like to thank the Brazilian agencies: São Paulo Research Foundation FAPESP (2012/02708-8; 2014/50869-6); National Council for Scientific and

Technological Development (CNPq) (process number: 465572/2014-6), and CAPES (Education Ministry) (23038.000776/201754 and Finance Code 001) via the projects of the National Institute for Science and Technology on Organic Electronics (INEO). This work was also developed within the scope of the project CICECO-Aveiro Institute of Materials, POCI-01-0145-FEDER-007679 (FCT Ref. UID/CTM/50011/2019) financed by Portuguese funds through the FCT/MEC and WINLEDs, POCI-01-0145-FEDER-030351. VT Freitas is acknowledged for the help in the PL measurements.

Data availability

The raw/processed data required to reproduce these findings cannot be shared at this time due to technical or time limitations.

References

[1] M. Fukuda, K. Sawada, K. Yoshino, Synthesis of Fusible and Soluble Conducting Polyfluorene Derivatives and Their Characteristics, Journal of Polymer Science Part a-Polymer Chemistry, 31 (1993) 2465-2471.

[2] Q. Pei, Y. Yang, Efficient photoluminescence and electroluminescence from a soluble polyfluorene. Journal of the American Chemical Society. 118 (1996) 7416-7417.

[3] X.M. Yu, G.J. Zhou, C.S. Lam, W.Y. Wong, X.L. Zhu, J.X. Sun, M. Wong, H.S. Kwok, A yellow-emitting iridium complex for use in phosphorescent multiple-emissive-layer white organic light-emitting diodes with high color quality and efficiency, Journal of Organometallic Chemistry, 693 (2008) 1518-1527.

[4] R.C. Evans, A.G. Macedo, S. Pradhan, U. Scherf, L.D. Carlos, H.D. Burrows, Fluorene Based Conjugated Polyelectrolyte/Silica Nanocomposites: Charge-Mediated Phase Aggregation at the Organic-Inorganic Interface. Advanced Materials, 22 (2010) 3032-3037.

[5] L.O. Péres, N. Errien, E. Faulques, H. Athalin, S. Lefran, F. Massuyeau, J. Wery, G. Froyer, S.H. Wang, Synthesis and characterization of a new alternating copolymer containing quaterphenyl and fluorenyl groups, Polymer. 48 (2007) 98-104.

[6] B. Liu, W.L. Yu, Y.H. Lai, W. Huang, Synthesis, characterization, and structure-property relationship of novel fluorene-thiophene-based conjugated copolymers, Macromolecules. 33 (2000) 8945-8952.

[7] R. Wang, W.Z. Wang, S. Lu, T. Liu, Controlled Radical Synthesis of Fluorene-Based Blue-Light-Emitting Copolymer Nanospheres with Core-Shell Structure via Self-Assembly, Macromolecules. 42 (2009) 4993-5000.

[8] J.H. Chen, C.S. Chang, Y.X. Chang, C.Y. Chen, H.L. Chen, S.A. Chen, Gelation and Its Effect on the Photophysical Behavior of Poly(9,9-dioctylfluorene-2,7-diyl) in Toluene, Macromolecules. 42 (2009) 1306-1314.

[9] I. Wang, E.B. Appert, O. Stéphan, A. Ibanez, P.L. Baldeck, Absorption and fluorescence properties of bifluorene crystal and microcrystals, Journal of Optics A-Pure and Applied Optics. 4 (2002) S258-S260.

[10] W.L. Yu, B. Liu, J. Pei, G. Zeng, W. Huang, Fluorene-based light-emitting polymers, Chinese Journal of Polymer Science. 19 (2001) 603-613.

[11] Z.Q. Lin, N.E. Shi, Y.B. Li, D. Qiu, L. Zhang, J.Y. Lin, J.F. Zhao, C. Wang, L.H. Xie, W. Huang, Preparation and Characterization of Polyfluorene-Based

Supramolecular pi-Conjugated Polymer Gels, Journal of Physical Chemistry C. 115 (2011) 4418-4424.

[12] X. Gong, P.K. Iyer, D. Moses, G.C. Bazan, A.J. Heeger, S.S. Xiao, Stabilized blue emission from polyfluorene-based light-emitting diodes: Elimination of fluorenone defects, Advanced Functional Materials. 13 (2003) 325-330.

[13] J.I. Lee, G. Klaerner, R.D. Miller, Oxidative stability and its effect on the photoluminescence of poly(fluorene) derivatives: End group effects. Chemistry of Materials. 11 (1999) 1083-1088.

[14] E.J.W. List, R. Guentner, P.S. Freitas, U. Scherf, The effect of keto defect sites on the emission properties of polyfluorene-type materials, Advanced Materials. 14 (2002) 374-378.

[15] E. Zojer, A. Pogantsch, E. Hennebicq, D. Beljonne, J.L. Brédas, E.J.W. List, Green emission from poly(fluorene)s: The role of oxidation. Journal of Chemical Physics. 117 (2002) 6794-6802.

[16] C. Chakraborty, P.K. Sukul, K. Dana, S. Malik, Suppression of Keto Defects and Thermal Stabilities of Polyfluorene-Kaolinite Clay Nanocomposites, Industrial & Engineering Chemistry Research. 52 (2013) 6722-6730.

[17] A. Miyao, Y. Mori, T. Uno, T. Itoh, T. Yamasaki, A. Koshio, M. Kubo, Incorporation of Fluorene-Based Emitting Polymers into Silica. Journal of Polymer Science Part A-Polymer Chemistry. 48 (2010) 5322-5328.

[18] M.C.C. Em, C.G. Barbosa, L.O. Péres, R. Faez, PF/CLAY hybrid materials: a simple method to modulate the optical properties, Polímeros. 26 (2016) 38-43.

[19] L.D. Carlos, Y. Messaddeq, H.F. Brito, R.A.S. Ferreira, V.Z. Bermudez, S.J.L. Ribeiro, Full-Color phosphors from Europium(III)-Based Organosilicates, Advanced Materials. 12 (2000) 594-598.

[20] C. Sanchez, B. Lebeau, F. Chaput, J.P. Boilot, Optical Properties of Functional Hybrid Organic-Inorganic Nanocomposites, Advanced Materials. 15 (2003) 1969-1994.

[21] S. Parola, B.J. López, L.D. Carlos, C. Sanchez, Optical Properties of Hybrid Organic-Inorganic Materials and their Applications, Advanced Functional Materials. 16 (2016) 6506-6544.

[22] F. Montilla, M.A. Cotarelo, E. Morallón, Hybrid sol-gel-conducting polymer synthesised by electrochemical insertion: tailoring the capacitance of polyaniline, Journal of Materials Chemistry. 19 (2009) 305-310.

[23] N. Willis-Fox, M. Kraft, J. Arlt, U. Scherf, R.C. Evans, Tunable White-Light Emission from Conjugated Polymer-Di-Ureasil Materials, Advanced Functional Materials. 26 (2016) 532-542.

[24] N.Willis-Fox, A.T. Marques, J. Arlt, U. Scherf, L.D. Carlos, H.D. Burrows, R.C. Evans, Synergistic photoluminescence enhancement in conjugated polymer-di-ureasil organic-inorganic composites, Chemical Science. 6 (2015) 7227-7237.

[25] I. Meazzini, C. Blayo, J. Arlt, A.T. Marques, U. Scherf, H.D. Burrows, R.C. Evans, Ureasil organic-inorganic hybrids as photoactive waveguides for conjugated polyelectrolyte luminescent solar concentrators, Materials Chemistry Frontiers. 11 (2017) 2271-2282.

[26] V.T. Freitas, L. Fu, A.M. Cojocariu, X. Cattoën, J. R. Bartlett, R. Le Parc, J.L. Bantignies, M.W.C, Man, P.S. André, R.A.S. Ferreira, L.D. Carlos, Eu^{3+} - Based

Bridged Silsesquioxanes for Transparent Luminescent Solar Concentrators, Applied Materials Interfaces. 7 (2015) 8770-8778.

[27] S.F.H. Correia, A. R. Frias, L. Fu, R. Rondão, E. Pecoraro, S.J.L. Ribeiro, P.S. André, R.A.S. Ferreira, L.D. Carlos, Large-Area Tunable Visible-to-Near-Infrared Luminescent Solar Concentrators, Advanced Sustainable Systems. 2 (2018) 1800002.

[28] A. Kaniyoor, B. McKenna, S. Comby, R.C. Evans, Design and Response of High – Efficiency, Planar , Doped Luminescent Solar Concentrators Using Organic – Inorganic Di-Ureasil Waveguides, Advanced Optical Materials. 4 (2016) 444-456.

[29] J.F.C.B. Ramalho, L.C.F. António, S.F.H. Correia, L.S. Fu, A.S. Pinho, C.D.S. Brites, L.D. Carlos, P.S. André, R.A.S. Ferreira, Luminescent QR codes for smart labelling and sensing, Optics and Laser Technology. 101 (2018) 304-311.

[30] A.R. Bastos, C.M.S. Vicente, R.O. Silva, N.J.O. Silva, M. Tacão, J.P. Costa, M. Lima, P.S. André, R.A.S. Ferreira, Integrated Optical Mach-Zehnder Interferometer Based on Organic -Inorganic Hybrids for Photonics-on-a-Chip Biosensing Applications, Sensors. 18 (2018) 840.

[31] X. Bai, G. Caputo, Z. Hao, V.T. Freitas, J. Zhang, R.L. Longo, O.L. Malta, R.A.S. Ferreira, N. Pinna, Efficient and tuneable photoluminescent boehmite hybrid nanoplates lacking metal activator centres for single-phase white LEDS, Nature Communications. 5 (2014) 5702.

[32] T. Suehiro, N. Hirosaki, R.J. Xie, T. Sato, Blue-emitting $LaSi_3N_5:Ce^{3+}$ fine powder phosphor for UV-converting white light-emitting diodos, Applied Physics Letters. 95 (2009) 051903.

[33] B. Li, X. Huang, J. Lin, Single-phased white-emitting $Ca_3Y(GaO)_3(BO_3)_4:Ce^{3+}$, Tb^{3+} , Sm^{3+} phosphors with high-efficiency: Photoluminescence , energy transfer and application in near-UV-pumped white LEDs, Journal of Luminescence. 204 (2018) 410-418.

[34] N.C. George, K.A. Denault, R. Seshadri, Phosphors for Solid-State White Lighting, Ann. Rev. Mater. Res. 43 (2013) 481-501.

[35] K. Takahashi, N. Hirosaki, R.J Xie, M. Harada, K.I Yoshimura, Y. Tomomura, Luminescence properties of blue $La_{1-x}Ce_xAl(Si_{6-z}Al_z)(N_{10-z}O_z)$ (z~1) oxynitride phosphors and their application in white light-emitting diode, Appl. Phys. Lett. 91 (2007) 091923.

[36] B. Dierre, R.J. Xie, N. Hirosaki, T. Sekiguchi, Blue emission of Ce^{3+} in lanthanide silicon oxynitride phosphors, J. Mater. Res. 22 (2007) 1933-1941.

[37] W. Xiao, X. Zhang, Z. Hao, G.H. Pan, Y. Luo, L. Zhang, J. Zhang. Blue-Emitting $K_2Al_2B_2O_7:Eu^{2+}$ Phosphor with High Thermal Stability and High Color Purity for Near-UV-Pumped White Light-Emitting Diodes, Inorg. Chem. 54 (2015) 3189-3195.

[38] T.C.F. Santos, L.O. Péres, S.H. Wang, O.N. Oliveira Jr, L. Caseli, Mixing Alternating Copolymers Containing Fluorenyl Groups with Phospholipids to Obtain Langmuir and Langmuir-Blodgett Films, Langmuir. 26 (2010) 5869–5875.

[39] V.Z. Bermudez, L.D. Carlos, L. Alcácer, Sol-gel derived urea cross-linked organically modified silicates. 1. Room temperature mid-infrared spectra, Chemistry of Materials. 11 (1999) 569-580.

[40] V.Z. Bermudez, R.A.S. Ferreira, L.D. Carlos, Coordination of Eu^{3+} ions in siliceous nanohybrids containing short polyether chains and bridging urea cross-links. Journal of Physical Chemistry B. 105 (2001) 3378-3386.

[41] C.G. Barbosa, R. Faez, L.O. Péres, Optical and Thermal Stability of Oligofluorene/Rubber Luminescent Blend, Journal of Fluorescence. 26 (2016) 1679-1684.

[42] M. Paris, L.O. Péres, O. Chauvet, G. Froyer, Solid-State NMR study of Na versus K doping of para-Phenylene oligomers. J. Phys. Chem. B 111 (2006) 743.

[43] P.P. Lima, R.A.S. Ferreira, S.A. Junior, O.L. Malta, L.D. Carlos, Terbium(III)-containing organic-inorganic hybrids synthesized through hydrochloric acid catalysis, Journal of Photochemistry and Photobiology A-Chemistry. 201 (2009) 214-221.

[44] W-L. Yu, Y. Cao, J. Pei, W. Huang, A. J. Heeger, Blue polymer light-emitting diodes from poly(9,9-dihexylfluorene-alt-co-2,5-didecyloxy-para-phenylene), Appl. Phys. Lett. 75, (1999) 3270.

[45] S.I. Hintschich, C. Rothe, S. Sinha, A.P. Monkman, Population and decay of keto states in conjugated polymers, J. Chem. Phys. 119 (2003) 12017.

- A UV-down shifting blue-emitting LED device was produced.
- Thermal stability of polyfluorene is due to interaction with di-ureasil hybrids.
- Maximum absolute emission quantum yield value for low polyfluorene concentration.